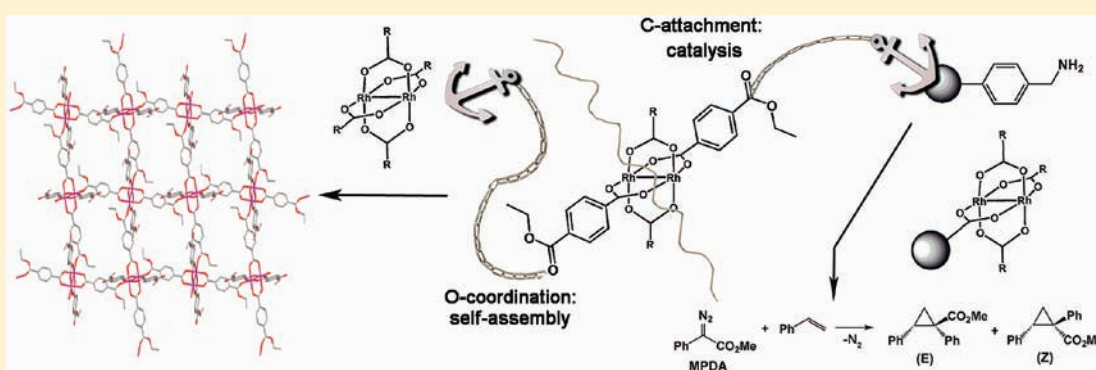


Dirhodium Paddlewheel with Functionalized Carboxylate Bridges: New Building Block for Self-Assembly and Immobilization on Solid Support

D. Krishna Kumar, Alexander S. Filatov, Margaret Napier, Jinyu Sun, Evgeny V. Dikarev, and Marina A. Petrukhina*

Department of Chemistry, University at Albany, 1400 Washington Avenue, Albany, New York 12222, United States

Supporting Information



ABSTRACT: A new dirhodium(II,II) paddlewheel complex, $[\text{Rh}_2(\text{O}_2\text{CC}_6\text{H}_4\text{COOC}_2\text{H}_5)_4]$ (**1**), has been synthesized using a pre-designed functionalized carboxylate, namely, 4-(ethoxycarbonyl)benzoate. The target product has been crystallized from the acetone solution and structurally characterized as a bis-acetone adduct, $[\text{Rh}_2(\text{O}_2\text{CC}_6\text{H}_4\text{COOC}_2\text{H}_5)_4(\text{OCMe}_2)_2] \cdot \text{C}_6\text{H}_{14}$ (**2**). By utilizing the ability of dangling ester groups to coordinate to open axial ends of neighboring dirhodium units, **1** can self-assemble to form 2D networks upon crystallization from solutions of noncoordinating solvents such as chlorobenzene and chloroform. The resulting $[\text{Rh}_2(\text{O}_2\text{CC}_6\text{H}_4\text{COOC}_2\text{H}_5)_4] \cdot 2\text{C}_6\text{H}_5\text{Cl}$ (**3**) and $[\text{Rh}_2(\text{O}_2\text{CC}_6\text{H}_4\text{COOC}_2\text{H}_5)_4] \cdot 2\text{CHCl}_3$ (**4**) products have microporous solid state structures with the pores filled with the corresponding disordered solvent molecules. Notably, **3** and **4** represent unique examples of 2D extended frameworks based on dirhodium tetracarboxylate paddlewheel units devoid of any exogenous ligands. In solution, the dangling ends of carboxylate bridges of **1** have been successfully utilized for condensation reaction with the selected solid support, benzylamine-functionalized polystyrene, allowing successful heterogenization of dirhodium units through the equatorial covalent attachment to the substrate. The resulting solid product was tested as a catalyst in the cyclopropanation reaction of styrene with methyl phenyldiazoacetate to show good yields and diastereoselectivity.

INTRODUCTION

Porous coordination polymers or metal–organic frameworks (MOFs) constructed from the assembly of organic linking units with metal ions or metal clusters constitute an exciting class of inorganic materials with unique properties and applications¹ such as gas storage, selective adsorption and separation of small molecules, ion exchange, and catalysis. A common strategy for assembling such frameworks is the use of multidentate organic linkers and metal-based secondary building units (SBUs) with linear, triangular, tetrahedral, square-planar, octahedral, and trigonal-prismatic geometries.² Paddlewheel metal complexes with multiply bonded dinuclear cores and rich redox properties³ have been broadly utilized as rigid linear building blocks for self-assembly reactions.^{4–6} Among those, dirhodium tetracarboxylates received considerable attention as very attractive linear units for formation of coordination networks with a variety of axially bound exogenous linkers.^{7,8} In this

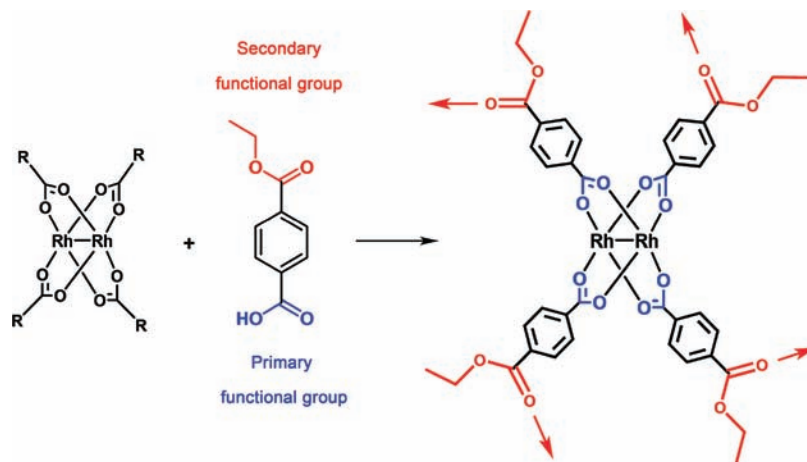
work, in order to support the dirhodium core we propose to utilize 4-(ethoxycarbonyl)benzoate (Scheme 1) having two different functions, such as carboxylic and ester groups.⁹ The target dirhodium(II,II) paddlewheel should be able to self-assemble without any additional linkers to form extended architectures, where porosity can be further tuned through specific guest inclusion or additional modification of benzoate bridges.

We also envision that the dangling ester ends of this complex can be used for a peptide-type covalent bond formation with functionalized solid supports to provide efficient heterogenization of pre-designed dimetal units. Recently, the use of solid support materials for grafting the rhodium-based catalysts¹⁰ has become an important new direction for increasing the

Received: February 20, 2012

Published: April 4, 2012

Scheme 1. Construction of Target Dirhodium Tetracarboxylate



durability of catalytic systems. The resulting heterogeneous catalysts are more stable and degrade much slower than their homogeneous counterparts; they are also reusable and allow the final products to be readily separated from the catalyst. Multiple efforts have been made to incorporate dirhodium(II) core complexes onto polymeric networks by various groups.¹¹ In our recent study, we explored a synthetic strategy based on grafting dirhodium(II,II) tetracarboxylates inside the functionalized channels of mesoporous silica having predesigned N-donor anchor sites and utilizing sufficiently strong noncovalent Rh...N interactions.¹² Herein, we extend these efforts to test the covalent bonding of dirhodium(II,II) paddlewheel complex onto a polymeric host, which should be a more efficient way to prepare recyclable and durable dirhodium-based catalysts for broad applications in organic synthesis.¹³

RESULTS AND DISCUSSION

The target tetrakis(4-ethoxycarbonylbenzoato)dirhodium(II,II) complex, $[\text{Rh}_2(\text{O}_2\text{CC}_6\text{H}_4\text{COOC}_2\text{H}_5)_4]$ (**1**), has been synthesized using a ligand-exchange procedure of tetrakis(trifluoroacetato)dirhodium(II,II)¹⁴ with 4-(ethoxycarbonyl)benzoic acid by reflux in chlorobenzene for 4 days in the presence of potassium carbonate and molecular sieves. ¹⁹F NMR spectra were used to monitor the reaction progress: the absence of a fluorine signal in a product indicated that all trifluoroacetate groups were substituted with benzoate ligands. Elemental analysis of the crude powder isolated from this reaction was also consistent with formation of a fully substituted product, $[\text{Rh}_2(\text{O}_2\text{CC}_6\text{H}_4\text{COOC}_2\text{H}_5)_4]$ (**1**). Slow evaporation of the solution of **1** in acetone/hexanes (10:3, v/v) afforded needle-shaped blue crystals of **2** in almost quantitative yield. Single-crystal X-ray diffraction analysis revealed that a bis-acetone adduct of **1**, $[\text{Rh}_2(\text{O}_2\text{CC}_6\text{H}_4\text{COOC}_2\text{H}_5)_4(\text{OCMe}_2)_2]\cdot\text{C}_6\text{H}_{14}$ (**2**), had been formed under these crystallization conditions. At the same time, the plate-shaped green crystals of $[\text{Rh}_2(\text{O}_2\text{CC}_6\text{H}_4\text{COOC}_2\text{H}_5)_4]\cdot 2\text{C}_6\text{H}_5\text{Cl}$ (**3**) have been grown from the chlorobenzene solution of **1** at elevated temperatures, while green blocks of $[\text{Rh}_2(\text{O}_2\text{CC}_6\text{H}_4\text{COOC}_2\text{H}_5)_4]\cdot 2\text{CHCl}_3$ (**4**) were obtained by slow diffusion of hexanes into a chloroform solution of **1** at ambient conditions. Single-crystal X-ray diffraction analyses established the 2D layered porous structures for both products **3** and **4** with the chlorobenzene and chloroform molecules occupying the pores, respectively.

Structural Description of $[\text{Rh}_2(\text{O}_2\text{CC}_6\text{H}_4\text{COOC}_2\text{H}_5)_4(\text{OCMe}_2)_2]\cdot\text{C}_6\text{H}_{14}$ (2**).** In the bis-adduct **2**, the acetone molecules are coordinated to both axial positions of the dirhodium(II,II) core (Figure 1), which is characteristic of

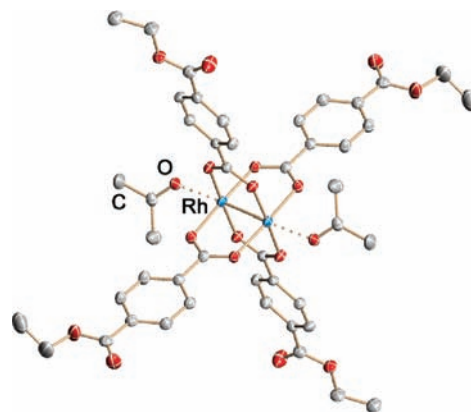


Figure 1. Molecular structure of $[\text{Rh}_2(\text{O}_2\text{CC}_6\text{H}_4\text{COOC}_2\text{H}_5)_4(\text{OCMe}_2)_2]\cdot\text{C}_6\text{H}_{14}$ (**2**) drawn with thermal ellipsoids at the 50% probability level. Hydrogen atoms and hexane molecules have been omitted for clarity. Acetone coordination to axial positions of a dirhodium unit is shown by dashed lines.

dimetal paddlewheel complexes crystallized from coordinating solvents. The Rh...O_{axial} distance of 2.276(1) Å is comparable to those usually found in dirhodium(II,II)-based adducts with axially bound acetone ligands (2.20–2.33 Å).^{7,8a} The Rh–Rh distance of 2.388(1) Å is within the range of 2.35–2.45 Å commonly observed in tetrakis(carboxylato)dirhodium(II,II) complexes.⁷ The Rh–O_{eq} distances span the range from 2.020(1) to 2.043(1) Å (Table 1).

In the solid state structure of **2**, there are solvent molecules of hexane occupying the interstitial space in the crystal lattice. Notably, the inability to form single crystals of **2**, when **1** is dissolved in neat acetone, demonstrates the necessity of a second solvent for crystallization. X-ray powder diffraction performed on bulk sample of **2** showed an excellent match with the simulated pattern, indicating the presence of a single phase. Thermal gravimetric analysis (TGA) of **2** reveals that the product loses both hexane and coordinated acetone molecules before 100 °C, while the complex starts to decompose at ca. 300 °C. X-ray powder diffraction (XRPD) analysis indicates

Table 1. Comparison of Selected Distances (Å) and Angles (deg) in $[\text{Rh}_2(\text{O}_2\text{CC}_6\text{H}_4\text{COOC}_2\text{H}_5)_4(\text{OCMe}_2)_2]\cdot\text{C}_6\text{H}_{14}$ (2), $[\text{Rh}_2(\text{O}_2\text{CC}_6\text{H}_4\text{COOC}_2\text{H}_5)_4]\cdot 2\text{C}_6\text{H}_5\text{Cl}$ (3), and $[\text{Rh}_2(\text{O}_2\text{CC}_6\text{H}_4\text{COOC}_2\text{H}_5)_4]\cdot 2\text{CHCl}_3$ (4)

	2	3	4
Rh–O _{eq}	2.020(1)–2.043(1)	2.024(4)–2.043(4)	2.021(3)–2.039(3)
Rh···O _{ax}	2.276(1)	2.306(4), 2.324(4)	2.272(3)
Rh–Rh	2.388(1)	2.387(1)	2.373(1)
Rh–Rh–O _{ax}	175.25(4)	174.09(10), 177.02(10)	176.83(5)

that the crystallinity of **2** is lost after drying the sample at 100 °C under vacuum for 12 h.

Structural Description of $[\text{Rh}_2(\text{O}_2\text{CC}_6\text{H}_4\text{COOC}_2\text{H}_5)_4]\cdot 2\text{C}_6\text{H}_5\text{Cl}$ (3). Single-crystal X-ray diffraction analysis revealed formation of a 2D layered network based on Rh···O_{ax} interactions between the rhodium centers and the carbonyl groups of dangling ester ends of carboxylate bridges. The Rh···O_{ax} contacts are 2.306(4) and 2.324(4) Å (Table 1). The Rh–O_{eq} distances are 2.024(4)–2.043(4) Å with the Rh–Rh bond length of 2.387(1) Å being the same as in **2**. Each dirhodium unit is connected to four other such units (Figure 2a).

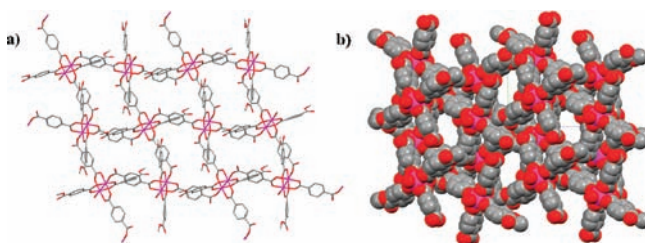


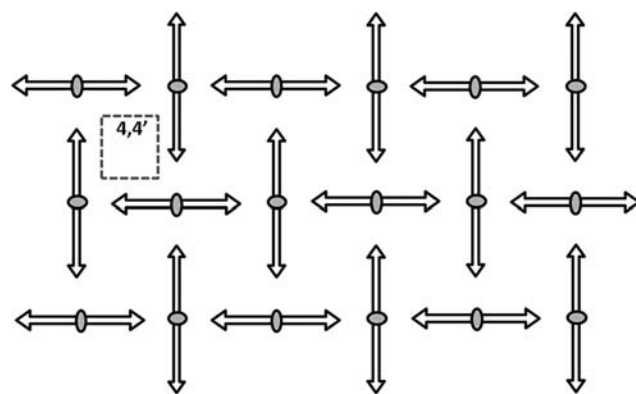
Figure 2. (a) Capped-stick representation of a single 2D layer in the crystal structure of $[\text{Rh}_2(\text{O}_2\text{CC}_6\text{H}_4\text{COOC}_2\text{H}_5)_4]\cdot 2\text{C}_6\text{H}_5\text{Cl}$ (3). (b) Space filling model of **3** showing the channels along the crystallographic *a* axis formed by an overlay of 2D layers.

While both Rh centers of a dimetal unit are engaged in intermolecular Rh···O axial interactions, not all four carboxylate groups are involved in network formation. Only two ligands that are positioned in a trans configuration to each other coordinate to metal centers. Considering dirhodium units as linear nodes, the overall topology can be described as a 4,4' sheet-like architecture (Scheme 2). The overlay of 2D coordination networks provides formation of channels running along the crystallographic *a* axis. These pores are parallel to the 2D layered networks (Figure 2b) and filled with the crystallization solvent molecules.

Crystals of **3** were subjected to thermal gravimetric analysis, showing that heating at 80 °C is sufficient to drive off the chlorobenzene molecules from the solid. Analysis shows no additional weight loss until the temperature reaches 340 °C, at which the weight loss of 70% is observed. XRPD analysis of **3** before and after heating revealed the loss of crystallinity upon evacuation of solvent, which is commonly observed in porous coordination polymers.¹⁵

Structural Description of $[\text{Rh}_2(\text{O}_2\text{CC}_6\text{H}_4\text{COOC}_2\text{H}_5)_4]\cdot 2\text{CHCl}_3$ (4). A 2D polymeric network based on Rh···O_{ax} interactions between the rhodium centers and the carbonyl groups of carboxylate bridges is constructed in a similar way as that in **3** (Figure 3a, Scheme 2). Rh–Rh and Rh···O_{ax} distances are 2.373(1) and 2.272(3) Å, respectively (Table 1). In contrast to **3**, the overlay of 2D layers in **4** provides a more complex porous network. There are two types

Scheme 2. Schematic Representation of the 2D Layer Formation in **3** and **4**^a



^aArrows and shadowed ellipsoids represent ester groups and dirhodium units, respectively. Arrow pointing toward the ellipsoid corresponds to the O coordination at the axial Rh site.

of continuous channels in the solid structure. One runs along the *c* axis and is filled with the CHCl_3 molecules (Figure 3b), while the other one remains free from solvent and extends along the [101] direction (Figure 3c), thus intersecting with the former at ca. 46.4°.

Formation of different pores in **3** and **4** can be attributed to the difference in size and shape of the guest chloroform and chlorobenzene molecules occupying the pores. The interconnected complex network in **4** has a noticeably larger solvent-accessible area (43.2%) compared to that in **3** (30.1%). Similarly to **2** and **3**, the solid sample of **4** is losing crystallinity upon removing solvent molecules. The phase purity of the bulk materials **3** and **4** was confirmed by comparing the experimental X-ray powder diffraction spectra with the simulated patterns based on single-crystal structural data (see Supporting Information, Figures S6 and S7).

Analysis of the Cambridge Structural Database (CSD) revealed that there are two cases¹⁶ where the axial positions of paddlewheel complexes are coordinated to the functional group of equatorial carboxylate ligands displaying a 1D polymeric structure. To the best of our knowledge, the new products **3** and **4** are the first examples of 2D networks built from dimetal paddlewheel units without employing exogenous linkers.

Grafting of **1 onto Solid Support.** Successful preparation of **1** along with the confirmation of its molecular structure allowed us to test the grafting of the predesigned dirhodium-(II,II) units onto a functionalized solid support. This was attempted via a peptide-type covalent linkage using the dangling ester ends of bridging carboxylate ligands of **1** (Scheme 3). This approach provides stronger binding to solid supports compared to axial coordination of dirhodium tetracarboxylate units that we explored recently.¹² For this

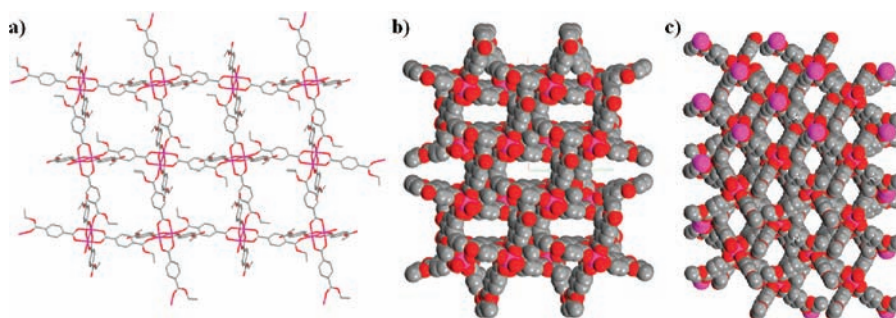
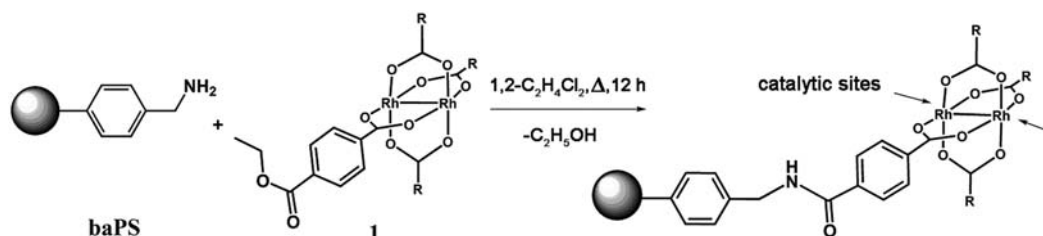


Figure 3. (a) Capped-stick representation of a single 2D layer in the crystal structure of $[\text{Rh}_2(\text{O}_2\text{CC}_6\text{H}_4\text{COOC}_2\text{H}_5)_4] \cdot 2\text{CHCl}_3$ (**4**). Space filling model showing the channels formed by an overlay of 2D layers running along the (b) crystallographic c axis and (c) $[101]$ direction.

Scheme 3. Grafting of 1 through the Condensation Reaction with Benzylamine-Functionalized Polystyrene (baPS) and Formation of an Amide Bond ($\text{R} = -\text{C}_6\text{H}_4\text{COOC}_2\text{H}_5$)

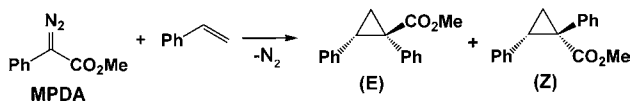


work, commercially available benzylamine-functionalized polystyrene (baPS) was selected as a recyclable support.¹⁷

Grafting was accomplished by heating the suspension of **1** with baPS in a freshly distilled 1,2-dichloroethane to produce a dark olive-green solid (**5**). Several solvents, including dichloromethane and chlorobenzene, were tested for grafting reaction, but 1,2-dichloroethane was found to be the preferred solvent media for heterogenization of **1**. The infrared (IR) spectrum of the grafted product exhibits a new peak at 1719 cm^{-1} in addition to the vibrational bands at 1724 (carboxylate) and 1689 cm^{-1} (ester) of the starting complex, thus illustrating formation of an amide bond. In the solid state UV-vis spectrum, a noticeable red shift of the absorption maximum of **1** after grafting also indicates successful heterogenization of dirhodium units.

Catalyst Evaluation. The catalytic properties of **5** were evaluated in the standard cyclopropanation reaction of methyl phenyldiazoacetate with styrene (Scheme 4) performed in

Scheme 4. Cyclopropanation of Styrene with Methyl Phenyldiazoacetate (MPDA)



hexanes under anhydrous conditions. For catalytic tests, a portion of **5** was suspended in hexanes and styrene and injected with a solution of methyl phenyldiazoacetate in hexanes at a rate of 0.7 mL/h . After 24 h of stirring at room temperature, the yield of cyclopropane was calculated by purification through a silica column using the solution of ethyl acetate in hexanes as an eluent. The isomer ratio was verified by ^1H NMR spectroscopy. It was found that cyclopropane is formed in 86% yield and 88% diastereomeric excess (de) after the first run. The catalyst efficiency was maintained over five repeated cycles (Table 2). Importantly, both the supernatant solution

Table 2. Catalytic Data for 5 in the Cyclopropanation Reaction of Styrene with MPDA

reaction cycle	ratio of isomers, % de	yield, %
1	88	86
2	88	81
3	88	81
4	88	74
5	88	76
6	88	64

and the solid host material (baPS) without grafted dirhodium complex show no catalytic activity in the above reaction.

For comparison, we tested the catalytic activity of **1** under homogeneous conditions and found it to produce cyclopropane in the same yield (85%) but with a slightly higher selectivity (96% de). Thus, immobilization of **1** onto baPS has not affected the catalytic activity of the dirhodium(II,II) complex.

In conclusion, the presence of two different functional groups makes the selected carboxylate ligand to be versatile for bridging a dinuclear metal core (through a primary carboxylate group) and allowing subsequent self-assembly or heterogenization of the resulting paddlewheel units through the secondary dangling group. In this work, the synthesis and full characterization of new tetrakis(4-ethoxycarbonylbenzoato)dirhodium(II,II) complex **1** have been successfully accomplished. X-ray crystallographic analysis of the bis-acetone adduct **2** confirmed the paddlewheel structure with the dirhodium core bridged by four carboxylic groups and having the ester ends free for secondary binding. These dangling ends of 4-(ethoxycarbonyl)benzoate ligands can be further utilized for self-assembly processes, as shown by formation of 2D networks **3** and **4** crystallized from chlorobenzene and chloroform, respectively. Interestingly, no examples of such self-assembly of dirhodium tetracarboxylate complexes have been found in the literature. Generally, strong σ -donating exogenous ligands are utilized for this purpose, allowing self-assembly of various extended

Table 3. Crystallographic Data and Structural Refinement Parameters for $[\text{Rh}_2(\text{O}_2\text{CC}_6\text{H}_4\text{COOC}_2\text{H}_5)_4(\text{OCMe}_2)_2] \cdot \text{C}_6\text{H}_{14}$ (2), $[\text{Rh}_2(\text{O}_2\text{CC}_6\text{H}_4\text{COOC}_2\text{H}_5)_4] \cdot 2\text{C}_6\text{H}_5\text{Cl}$ (3), and $[\text{Rh}_2(\text{O}_2\text{CC}_6\text{H}_4\text{COOC}_2\text{H}_5)_4] \cdot 2\text{CHCl}_3$ (4)

	2	3	4
empirical formula	$\text{C}_{52}\text{H}_{62}\text{O}_{18}\text{Rh}_2$	$\text{C}_{52}\text{H}_{46}\text{Cl}_2\text{O}_{16}\text{Rh}_2$	$\text{C}_{42}\text{H}_{38}\text{Cl}_6\text{O}_{16}\text{Rh}_2$
fw	1180.84	1203.61	1217.24
cryst syst	monoclinic	monoclinic	monoclinic
space group	$P2_1/n$	$P2_1/n$	$C2/c$
<i>a</i> (Å)	9.8635(13)	12.6460(10)	22.3558(15)
<i>b</i> (Å)	13.1392(17)	16.2693(12)	16.8627(11)
<i>c</i> (Å)	20.333(3)	25.792(2)	16.4080(11)
α (°)	90.00	90.00	90.00
β (°)	94.940(2)	103.8910(10)	92.8000(10)
γ (°)	90.00	90.00	90.00
<i>V</i> (Å ³)	2625.4(6)	5151.3(7)	6178.1(7)
<i>Z</i>	2	4	4
<i>D</i> _{calcd} (g/cm ³)	1.494	1.552	1.309
<i>F</i> (000)	1216	2440	2440
μ (mm ⁻¹)	0.701	0.814	0.847
temp. (K)	100(2)	173(2)	100(2)
reflns collected/unique/obsd [<i>I</i> > 2σ(<i>I</i>)]	19 722/5151/4719	40 083/10176/5864	23 277/6078/5125
data/restraints/parameters	5151/0/330	10176/24/665	6078/0/309
<i>R</i> 1, ^a <i>wR</i> 2 ^b [<i>I</i> > 2σ(<i>I</i>)]	0.0279, 0.0731	0.0600, 0.1109	0.0341, 0.0978
<i>R</i> 1, ^a <i>wR</i> 2 ^b (all data)	0.0307, 0.0754	0.1211, 0.1332	0.0414, 0.1005
quality of fit ^c	1.069	1.022	1.195
largest diff. peak/hole (e/Å ³)	0.989/−0.291	1.297/−1.006	1.301/−0.747

^a*R*1 = $\sum||F_o| - |F_c|| / \sum|F_o|$. ^b*wR*2 = $[\sum[w(F_o^2 - F_c^2)^2] / \sum[w(F_o^2)^2]]^{1/2}$. ^cQuality of fit = $[\sum[w(F_o^2 - F_c^2)^2] / (N_{\text{obs}} - N_{\text{params}})]^{1/2}$, based on all data.

networks through intermolecular axial coordination to open metal sites of paddlewheel units. Complex **1** was also successfully immobilized onto an amine-functionalized solid substrate using the peptide-type bond condensation reaction. The resulting dirhodium-based solid product was tested as a heterogeneous catalyst in the model diazo decomposition reaction in the presence of styrene. The catalyst was recycled and reused through several consequent runs to show good catalytic activity by providing a mixture of cyclopropanes with high yields and diastereoselectivity.

EXPERIMENTAL SECTION

Materials and Methods. All manipulations were carried out under an oxygen-free, dinitrogen atmosphere by employing standard glovebox and Schlenk techniques. All chemicals were reagent grade and used as received without further purification. Anhydrous solvents were obtained from a Solvent Purification System purchased from M. Braun, Inc., USA, or freshly distilled according to published methods.¹⁸ Additionally, toluene and hexanes were dried over Na/benzophenone and distilled prior to use. 1,2-Dichloroethane was refluxed over CaCl_2 and fractionally distilled. Tetrakis(trifluoroacetato)dirhodium(II,II) was synthesized according to the reported procedure.¹⁴ Benzylamine-functionalized polystyrene (baPS) was purchased from Alfa Aesar. Molecular sieves and potassium carbonate were activated at 125 °C for 3 days prior to use.

The attenuated total reflection (ATR) IR spectra were recorded on a Perkin-Elmer Spectrum 100 FT-IR spectrometer. NMR spectra were obtained using a Bruker Avance 400 spectrometer at 400 MHz for ¹H and at 376.47 MHz for ¹⁹F. Chemical shifts (δ) are reported in ppm relative to residual solvent peaks for ¹H and to CFCl_3 for ¹⁹F. Elemental analyses were performed by Guelph Chemical Laboratories, Ltd., Canada. Thermogravimetric measurements were carried out under $\text{N}_2(\text{g})$ at a heating rate of 5 °C/min using a TGA 2050 Thermogravimetric Analyzer, TA Instruments. X-ray data were collected at −100 or −173 °C (Bruker KYRO-FLEX) on a Bruker APEX CCD X-ray diffractometer equipped with graphite-monochromated Mo *K*α radiation (λ = 0.71073 Å) operated at 1800 W power.

Single crystals were selected and mounted on a goniometer head with silicone grease. Frames were integrated with the Bruker SAINT software package,¹⁹ and structures were solved and refined using Bruker SHELXTL (version 6.12) software.²⁰ Crystallographic data and refinement parameters for 2–4 are listed in Table 3. X-ray powder diffraction data were collected on a Bruker D8 Advance diffractometer (Cu *K*α radiation, focusing Göbel Mirror, LynxEye one-dimensional detector, step of 0.02° 2θ, 20 °C). Crystalline samples under investigation were ground and placed in an airtight holder with a plastic dome cover under an atmosphere of $\text{N}_2(\text{g})$.

Synthesis of 4-(Ethoxycarbonyl)benzoic Acid. Diethyl terephthalate (2.2 g, 10 mmol) was dissolved in 30 mL of ethanol by stirring for 15 min with gentle heating. Potassium hydroxide (580 mg, 10 mmol) was added, and the previously clear solution slowly became cloudy. The mixture was refluxed for 4 h, cooled, and evaporated to dryness. The resulting product was then suspended in water and extracted with dichloromethane. The aqueous layer was collected and acidified with a 10% solution of hydrochloric acid to yield a colorless precipitate. The product was extracted with ethyl ether 3 times, dried over sodium sulfate, and decanted. Ether was removed by evaporation under vacuum to afford a white solid. To recrystallize the product, it was dissolved in dichloromethane and filtered through a Buchner funnel. The solution was collected, reduced to ~30 mL, and left for slow evaporation. Colorless crystals deposited in 2 days. They were collected, washed in cold dichloromethane, and dried. Yield: 1.01 g, 53%. ¹H NMR (CDCl_3 , 22 °C, ppm): δ = 12.42 (s, 1H), 8.20–8.14 (m, 4H), 4.46–4.40 (q, 2H), 1.45–1.41 (t, 3H).

Synthesis of Tetrakis(4-ethoxycarbonylbenzoato)dirhodium(II,II), $[\text{Rh}_2(\text{O}_2\text{CC}_6\text{H}_4\text{COOC}_2\text{H}_5)_4]$ (1). Activated 4 Å molecular sieves (6.0 g) and dried potassium carbonate (0.537 g) were wrapped separately and placed in the thimble of a Soxhlet extractor. Chlorobenzene (150 mL) was added to tetrakis(trifluoroacetato)dirhodium(II,II) (0.200 g, 0.30 mmol) and 4-(ethoxycarbonyl)benzoic acid (0.300 g, 1.5 mmol) in a 250 mL Schlenk flask. The flask was connected to the Soxhlet extractor under a dinitrogen atmosphere and refluxed for 5 days at 150–160 °C. The resulting solution was evaporated to dryness to afford a light-green solid. Crude product was washed with 10 mL of a solution of hexanes/dichloromethane (10:1, v/v) and dried under reduced pressure to

yield a fine green powder of **1**. Yield: 0.261 g, 89%. Anal. Calcd for $C_{40}H_{36}O_{16}Rh_2$: C, 49.10; H, 3.71; O, 26.16. Found: C, 49.13; H, 3.71; O, 29.10. ^{19}F NMR (400 MHz, $(CD_3)_2CO$, 22 °C): no signal. 1H NMR ($(CD_3)_2CO$, 22 °C, ppm): δ = 8.00–7.93 (m, 4H) 4.34–4.29 (q, 2H), 1.35–1.31 (t, 3H). FT-IR (cm^{-1}): 1724m, 1689m, 1602m, 1560m, 1507w, 1396s, 1370m, 1259s, 1172m, 1141m, 1100s, 1016s, 880m, 838m, 797s, 736s, 713s. UV–vis (chloroform, 22 °C, λ_{max} nm (ϵ , $M^{-1} cm^{-1}$)): 456 (81), 604 (94). UV–vis (chlorobenzene, 22 °C, λ_{max} nm (ϵ , $M^{-1} cm^{-1}$)): 660 (613). UV–vis (solid, 22 °C, λ_{max} nm): 523.

Synthesis of $[Rh_2(O_2CC_6H_4COOC_2H_5)_4(OCMe_2)_2] \cdot C_6H_{14}$ (2**).** A portion of **1** (0.020 g, 0.02 mmol) was dissolved in 7 mL of acetone and 3 mL of hexanes and left for slow evaporation in air. In 2 days, dark-blue crystals of **2** appeared. Yield: 0.021 g, 83%. Anal. Calcd for $C_{52}H_{62}O_{18}Rh_2$: C, 52.89; H, 5.29; O, 24.39. Found: C, 52.69; H, 5.42; O, 24.10. 1H NMR ($CDCl_3$, 22 °C, ppm): δ = 8.00–7.91 (m, 16H), 4.36–4.30 (q, 8H), 2.50 (s, 12H), 1.37–1.27 (m, 12H), 0.90–0.87 (m, 14H). FT-IR (cm^{-1}): 2957w, 2925w, 2856w, 2161w, 1978w, 1719m, 1707m, 1683m, 1604m, 1560m, 1506w, 1472w, 1422w, 1393s, 1366s, 1261s, 1174w, 1140m, 1105s, 1018s, 881w, 837m, 800w, 737s, 715m. UV–vis (acetone, 22 °C, λ_{max} nm (ϵ , $M^{-1} cm^{-1}$)): 458 (115), 595 (177).

Crystal Growth of $[Rh_2(O_2CC_6H_4COOC_2H_5)_4] \cdot 2C_6H_5Cl$ (3**).** A portion of **1** (0.010 g, 0.01 mmol) was placed in a 12.7 mm glass ampule, to which 6 mL of anhydrous chlorobenzene was added. The system was sealed and heated to ca. 100 °C. Green plate-like crystals of **3** were deposited on the sides of the ampule in 3 days.

Crystal Growth of $[Rh_2(O_2CC_6H_4COOC_2H_5)_4] \cdot 2CHCl_3$ (4**).** A portion of **1** (0.020 g, 0.02 mmol) was dissolved in 4 mL of anhydrous chloroform. This solution was carefully layered with 2 mL of anhydrous hexanes and kept for crystallization. Green blocks of **4** were deposited in 3 days.

Grafting of **1 onto Benzylamine-Functionalized Polystyrene.** Grafting was done by dissolving a portion of **1** (0.040 g, 0.04 mmol) in 15 mL of the freshly distilled 1,2-dichloroethane to produce a transparent green solution which was then mixed with white beads of benzylamine on polystyrene (baPS) (0.100 g, 0.20–0.30 mmol active sites). After 20 min of heating, the polymer beads started to darken in color. The suspension was refluxed for 12 h. The resulting olive-green solid (**5**) was separated from solution by cannula filtration and washed at least 3 times in 10 mL of freshly distilled acetone or dichloromethane, which remained colorless.

The olive-green solid was dried overnight in a ca. 70 °C sand bath in vacuo. Yield: 0.140 g, 100% (based on initial amount of Rh). FT-IR (cm^{-1}): 2960w, 2928w, 2860w, 2161w, 1978w, 1721m, 1595w, 1558w, 1507w, 1493w, 1453w, 1393w, 1260m, 1119w, 1102w, 1071w, 1017w, 876w, 836w, 798w, 737m, 714w, 699w. UV–vis (solid, before catalysis, 22 °C, λ_{max} nm): 592. UV–vis (solid, after 6 catalytic cycles, 22 °C, λ_{max} nm): 533.

Catalyst Evaluation Details. Solutions of methyl phenyl-diazoacetate (MPDA) (0.02 g/mL) and styrene (0.1 g/mL) were prepared in hexanes and degassed three times. A solution of styrene (6 mL) was added to 0.015 g of the catalyst and stirred at room temperature for 30 min. A solution of MPDA (3 mL) was added using a syringe pump at a rate of 0.70 mL/h. The temperature of the MPDA solution was kept at 6 °C throughout addition. The mixture was stirred for 24 h at room temperature. After completion of the reaction, the suspension was transferred to a centrifuge tube (under inert atmosphere) and centrifuged. The supernatant liquid was removed via a cannula, and 20 mL of anhydrous hexanes was added to the remaining solid. The obtained suspension was sonicated and centrifuged again. Extraction of the products was repeated twice. The hexanes portions were combined, dried, and subjected to column chromatography (EtOAc/hexanes). The product (mixture of isomers) was collected, and 1H NMR spectra were recorded to calculate the yield using dimethyl aminopyridine (DMAP) as an internal standard. Leaching of the catalyst **5** has been monitored by 1H NMR spectroscopy. After completion of the selected catalytic cycle, the reaction mixture was separated from the catalyst by filtration, evaporated to dryness, and then redissolved. Analysis of the 1H

NMR spectra revealed the absence of any traces of carboxylate ligands, showing the sufficient stability of the heterogeneous catalyst.

■ ASSOCIATED CONTENT

📄 Supporting Information

CIF files providing crystallographic data for compounds **2–4**; X-ray powder patterns and TGA plots for **2–4**. This material is available free of charge via the Internet at <http://pubs.acs.org>.

■ AUTHOR INFORMATION

Corresponding Author

*E-mail: mpetrukhina@albany.edu.

Notes

The authors declare no competing financial interest.

■ ACKNOWLEDGMENTS

We thank the National Science Foundation, CHE-1152441 (ED) and CHE-0546945 (MP), for support of this work. We are also grateful to the University at Albany for supporting the X-ray Center at the Department of Chemistry.

■ REFERENCES

- (1) (a) James, S. L. *Chem. Soc. Rev.* **2003**, *32*, 276–288. (b) Rowsell, L. C.; Yaghi, O. M. *Microporous Mesoporous Mater.* **2004**, *73*, 3–14. (c) Fujita, M.; Tominaga, M.; Hori, A.; Therrien, B. *Acc. Chem. Res.* **2005**, *38*, 369–378. (d) Lin, W. J. *Solid State Chem.* **2005**, *178*, 2486–2490. (e) Kitagawa, S.; Noro, S.; Nakamura, T. *Chem. Commun.* **2006**, 701–707. (f) Mueller, U.; Schubert, M.; Teich, F.; Puetter, H.; Schierle-Arndt, K.; Pastre, J. *J. Mater. Chem.* **2006**, *16*, 626–636. (g) Lin, X.; Jia, J.; Hubberstey, P.; Schroder, M.; Champness, N. R. *CrystEngComm* **2007**, *9*, 438–448. (h) Dincă, M.; Long, J. R. *J. Am. Chem. Soc.* **2007**, *129*, 11172–11176. (i) Morris, R. E.; Wheatley, P. S. *Angew. Chem., Int. Ed.* **2008**, *47*, 4966–4981. (j) Tanaka, D.; Kitagawa, S. *Chem. Mater.* **2008**, *20*, 922–931. (k) Banerjee, R.; Furukawa, H.; Britt, D.; Knobler, C.; O’Keeffe, M.; Yaghi, O. M. *J. Am. Chem. Soc.* **2009**, *131*, 3875–3877. (l) Northrop, B. H.; Zheng, Y.-R.; Chi, K.-W.; Stang, P. J. *Acc. Chem. Res.* **2009**, *42*, 1554–1563. (m) Klosterman, J. K.; Yamauchi, Y.; Fujita, M. *Chem. Soc. Rev.* **2009**, *38*, 1714–1725. (n) Chakrabarty, R.; Mukherjee, P. S.; Stang, P. J. *Chem. Rev.* **2011**, *111*, 6810–6918.
- (2) (a) Yaghi, O. M.; O’Keeffe, M.; Ockwig, N. W.; Chae, H. K.; Eddaoudi, M.; Kim, J. *Nature* **2003**, *423*, 705–714. (b) Ockwig, N. W.; Delgado-Friedrichs, O.; O’Keeffe, M.; Yaghi, O. M. *Acc. Chem. Res.* **2005**, *38*, 176–182. (c) Férey, G. *Chem. Soc. Rev.* **2008**, *37*, 191–214.
- (3) In *Multiple Bonds Between Metal Atoms*, 3rd ed.; Cotton, F. A., Murillo, C. A., Walton, R. A., Eds.; Springer Science and Business Media Inc.: New York, 2005.
- (4) (a) Mori, W.; Takamizawa, S.; Kato, C. N.; Ohmura, T.; Sato, T. *Microporous Mesoporous Mater.* **2004**, *73*, 31–46. (b) Takamizawa, S.; Nakata, E.; Saito, T.; Akatsuka, T. *Inorg. Chem.* **2005**, *44*, 1362–1366. (c) Ueda, T.; Takahiro, K.; Eguchi, T.; Kachi-Terajima, C.; Takamizawa, S. *J. Phys. Chem. C* **2007**, *111*, 1524–1534. (d) Takamizawa, S.; Nataka, E.-I.; Akatsuka, T.; Miyake, R.; Kakizaki, Y.; Takeuchi, H.; Maruta, G.; Takeda, S. *J. Am. Chem. Soc.* **2010**, *132*, 3783–3792. (e) Chen, M.-S.; Chen, M.; Takamizawa, S.; Okamura, T.-A.; Fan, J.; Sun, W.-Y. *Chem. Commun.* **2011**, *47*, 3787–3789.
- (5) (a) Wesemann, J. L.; Chisholm, M. H. *Inorg. Chem.* **1997**, *36*, 3258–3267. (b) Rusjan, M.; Donnio, B.; Guillon, D.; Cukiernik, F. D. *Chem. Mater.* **2002**, *14*, 1564–1575. (c) Chisholm, M. H.; Patmore, N. J. *Acc. Chem. Res.* **2007**, *40*, 19–27. (d) Chisholm, M. H.; Dann, A. S.; Dielmann, F.; Gallucci, J. C.; Patmore, N. J.; Ramnauth, R.; Scheer, M. *Inorg. Chem.* **2008**, *47*, 9248–9255.
- (6) (a) Cotton, F. A.; Lin, C.; Murillo, C. A. *Acc. Chem. Res.* **2001**, *34*, 759–771. (b) Cotton, F. A.; Dikarev, E. V.; Petrukhina, M. A. *Angew. Chem., Int. Ed.* **2000**, *39*, 2362–2364. (c) Bera, J. K.; Angaridis, P. A.;

Petrukhina, M. A.; Cotton, F. A.; Fanwick, P. E.; Walton, R. A. *J. Am. Chem. Soc.* **2001**, *123*, 1515–1516. (d) Cotton, F. A.; Dikarev, E. V.; Petrukina, M. A. *Angew. Chem., Int. Ed.* **2001**, *40*, 1521–1523. (e) Cotton, F. A.; Hillard, E. A.; Murillo, C. A. *J. Am. Chem. Soc.* **2002**, *124*, 5658–5660. (f) Cotton, F. A.; Lin, C.; Murillo, C. A. *Proc. Natl. Acad. Sci.* **2002**, *99*, 4810–4813.

(7) Chifotides, H. T.; Dunbar, K. R. Rhodium Compounds. In *Multiple Bonds between Metal Atoms*, 3rd ed.; Cotton, F. A., Murillo, C. A., Walton, R. A., Eds.; Springer Science and Business Media Inc.: New York, 2005; pp 465–589.

(8) (a) Dikarev, E. V.; Andreini, K.; Petrukina, M. A. *Inorg. Chem.* **2004**, *43*, 3219–3224. (b) Petrukina, M. A.; Scott, L. T. *Dalton Trans.* **2005**, 2969–2975. (c) Petrukina, M. A.; Andreini, K.; Tsefrikas, V. M.; Scott, L. T. *Organometallics* **2005**, *24*, 1394–1397. (d) Filatov, A. S.; Rogachev, A. Yu.; Petrukina, M. A. *Cryst. Growth Des.* **2006**, *6*, 1479–1484. (e) Petrukina, M. A. *Coord. Chem. Rev.* **2007**, *251*, 1690–1698. (f) Filatov, A. S.; Petrukina, M. A. *Coord. Chem. Rev.* **2010**, *254*, 2234–2246.

(9) Chenot, E.-D.; Bernardi, D.; Comel, A.; Kirsch, G. *Synth. Commun.* **2007**, *37*, 483–490.

(10) (a) Bluemel, J. *Coord. Chem. Rev.* **2008**, *252*, 2410–2423. (b) Guenther, J.; Reibenspies, J.; Bluemel, J. *Adv. Synth. Catal.* **2011**, *353*, 443–460.

(11) (a) Doyle, M. P.; Timmons, D. J.; Tumonis, J. S.; Gau, H.-M.; Blosser, E. C. *Organometallics* **2002**, *21*, 1747–1749. (b) Davies, H. M. L.; Walji, A. M. *Org. Lett.* **2003**, *5*, 479–482. (c) Davies, H. M. L.; Walji, A. M.; Nagashima, T. *J. Am. Chem. Soc.* **2004**, *126*, 4271–4280. (d) Hulman, H. M.; de Lang, M.; Arends, I. W. C. E.; Hanefeld, U.; Sheldon, R. A.; Maschmeyer, T. *J. Catal.* **2003**, *217*, 264–274. (e) Takeda, K.; Oohara, T.; Anada, M.; Nambu, H.; Hashimoto, S. *Angew. Chem., Int. Ed.* **2010**, *49*, 6979–6983.

(12) Dikarev, E. V.; K. Kumar, D.; Filatov, A. S.; Anan, A.; Xie, Y.; Asefa, T.; Petrukina, M. A. *ChemCatChem* **2010**, *2*, 1461–1466.

(13) (a) Doyle, M. P.; McKervey, M. A.; Ye, T. In *Modern Catalytic Methods for Organic Synthesis with Diazo Compounds*; Wiley-Interscience: New York, 1998. (b) Davies, H. M. L.; Hedley, S. J. *Chem. Soc. Rev.* **2007**, *36*, 1109–1119. (c) Hansen, J.; Davies, H. M. L. *Coord. Chem. Rev.* **2008**, *152*, 545–555. (d) Davies, H. M. L.; Denton, J. R. *Chem. Soc. Rev.* **2009**, *38*, 3061–3071. (e) Doyle, M. P.; Duffy, R.; Ratnikov, M.; Zhou, L. *Chem. Rev.* **2010**, *110*, 704–724.

(14) Cotton, F. A.; Dikarev, E. V.; Feng, X. *Inorg. Chim. Acta* **1995**, *237*, 19–26.

(15) Dikarev, E. V.; Li, B.; Chernyshev, V. V.; Shpanchenko, R. V.; Petrukina, M. A. *Chem Commun.* **2005**, 3274–3276.

(16) A CSD analysis performed for a transition-metal-based paddlewheel core bridged by four benzoate ligands (leaving five C atoms of the benzene ring open) resulted in 695 hits. Analysis of the results revealed that there are two cases where the axial positions of paddlewheel complexes are coordinated to the functional group of the equatorial carboxylate ligand. First, the 1D polymeric chain was formed when the axial positions of dicopper(II) paddlewheel units are coordinated to the N atoms of bridging 3-cyano benzoate ligands. Cueto, S.; Rys, P.; Straumann, H.-P.; Gramlich, V.; Rys, F. S. *Acta Crystallogr.* **1992**, *C48*, 2122–2124. Second, a dimolybdenum(II) paddlewheel is coordinated to the O atoms of 4-diphenylphosphinylbenzoate bridging ligands, also displaying a 1D propagation mode. Kuang, S.-M.; Fanwick, P. E.; Walton, R. A. *Inorg. Chem. Commun.* **2002**, *5*, 134–138. Although the authors reported the structure as a 2D network, the propagation mode is one dimensional. There are also structures of polymeric networks with ligands having different functionality, but the frameworks are comprised of two different metal units, for example, (a) a paddlewheel and square pyramidal copper unit or (b) a paddlewheel and triangular planar copper unit. (a) McManus, G. J.; Wang, Z.; Beauchamp, D. A.; Zaworotko, M. J. *Chem. Commun.* **2007**, 5212–5213. (b) Wen, Y.-H.; Cheng, J.-K.; Zhang, J.; Li, Z.-J.; Kang, Y.; Yao, Y.-G. *Inorg. Chem. Commun.* **2004**, *7*, 1120–1123.

(17) McNamara, C. A.; Dixon, M. J.; Bradley, M. *Chem. Rev.* **2002**, *102*, 3275–3300.

(18) Perrin, D. D.; Armarego, L. F.; Perrin, D. R. *Purification of Laboratory Chemicals*, 2nd ed.; Pergamon Press, Oxford: New York, 1980.

(19) SAINT, version 6.02; Bruker AXS, Inc.: Madison, WI, 2001. SADABS; Bruker AXS, Inc.: Madison, WI, 2001.

(20) (a) Sheldrick, G. M. *Acta Crystallogr.* **2008**, *A64*, 112–122. (b) SHELXTL, version 6.14; Bruker AXS, Inc.: Madison, WI, 2001.